






Meta-Material Topology Optimization with Geometric Control

Jikai Liu¹ , Jinyuan Tang² , Rafiq Ahmad³  and Yongsheng Ma⁴ 

¹University of Pittsburgh, jil220@pitt.edu

²Central South University, jytangcsu@163.edu

³University of Alberta, rafiq@ualberta.ca

⁴University of Alberta, yongsheng.ma@ualberta.ca

Corresponding author: Yongsheng Ma, yongsheng.ma@ualberta.ca

ABSTRACT

This paper explores the geometric control techniques in meta-material topology optimization. Specifically, the component length scale control technique was applied to constrain the minimum structural member size to be larger than the printing resolution; the curvature control was employed to round off the sharp corners so that to reduce the stress concentration and improve the fatigue resistance. Beyond the single material unit design, the proposed techniques were also applied to the meta-material optimization given a part-scale circumstance, where the micro/meso-scale structural details were optimized to fit the part-scale loading condition. A few numerical examples were studied to prove the effectiveness of the proposed techniques.

Keywords: Meta-Material, Topology Optimization, Manufacturability, Length Scale Control, Curvature control

DOI: <https://doi.org/10.14733/cadaps.2019.951-961>

1 INTRODUCTION

Topology optimization is a numerical optimization method to design lightweight, superior performing mechanical structures. With the intensive development during the last a few decades, topology optimization has been proved as an effective and robust tool in designing mechanical structures subject to a variety of physical discipline, e.g., solid mechanics, fluid dynamics, and thermal dynamics, etc [2]. Especially with the many manufacturability-related issues being addressed [6,16], topology optimization now has been widely accepted for industrial applications.

Other than the part scale applications, meta-material design through topology optimization has recently been focused [3,13], since extraordinary mechanical properties can be achieved such as negative Poisson's ratio and negative thermal expansion. Here, meta-material means architected material engineered to have certain property which does not exist in nature. These days, advancement of additive manufacturing (AM) technology makes fabrication of the designed meta-

materials no longer a tough issue, as demonstrated in literature [9,11]. And under the AM background, unit cell of the meta-material is often at the millimeter level (such as 1~3mm) so that it can be fabricated out in good geometric form and also being self-support. Even though meta-material topology optimization has demonstrated the promise, there are still key issues to be addressed to further improve the performance and enhance the manufacturability, which are specified below:

- (1) Manufacturability issues still exist in meta-material AM and should be carefully addressed when developing the related optimization algorithm, e.g, the structural members should have the size larger than the AM printing resolution which otherwise cannot be successfully printed. Hence, in this article, the key problem of component length scale control will be discussed and addressed.
- (2) To improve the fatigue resistance of the meta-material formed structure, it is better to eliminate the sharp reentrant corners which are prone of stress concentration. This issue will be addressed by constraining curvatures of the concave boundary areas, because performing stress constrained optimization at the meta-material level is non-trivial.
- (3) Mutli-scale topology optimization is important since all the meta-material design techniques will finally be applied in the part-scale circumstance. Hence, a few part-scale design examples will be studied in this research by including the afore-mentioned geometric control techniques.

So far, SIMP (Solid Isotropic Material with Penalization) [2], level set [1,12], and ESO (Evolutionary Structural Optimization) [15] are the main-stream topology optimization methods. From the authors' opinion, level set method has the strongest capability in supporting geometric control since it employs the boundary contour-based structural evolution which can always capture the clear-cut structural boundary and access the related high-order geometric information [1,12]. Therefore, level set method will be employed in this study so that to better solve the afore-mentioned geometric control issues. To better under level set method, a comprehensive literature survey can be found in [10].

2 METHOD DESCRIPTION AND CASE STUDY

2.1 Level set method

Level set function $\Phi(\mathbf{X}): R^n \mapsto R$, represents any structure in the implicit form, as:

$$\begin{cases} \Phi(\mathbf{X}) > 0, & \mathbf{X} \in \Omega / \partial\Omega \\ \Phi(\mathbf{X}) = 0, & \mathbf{X} \in \partial\Omega \\ \Phi(\mathbf{X}) < 0, & \mathbf{X} \in D/\Omega \end{cases} \quad (2.1)$$

where Ω represents the material domain, D indicates the entire design domain, and thus D/Ω represents the void.

Generally, the level set field satisfies the signed distance regulation through solution of Eqn. (2.2), where absolute of the level set value at any point represents its shortest distance to the structural boundary and the sign indicates the point to be either solid (> 0), or void (< 0).

$$|\nabla\Phi(\mathbf{X})| = 1 \quad (2.2)$$

In the structural optimization background, the optimization problem is formulated based on the level set function which is then solved to derive the boundary velocity field. The boundary velocities will be used to update the zero-value level set contour, i.e. the structural boundary, which in the classic method is conducted by solving the Hamilton-Jacobi equation. In this way, the structural boundary will be gradually evolved in an iterative manner till convergence of the optimization problem.

2.2 Meta-material Optimization problem

Meta-material optimization means the design of material distribution with in a RVE (representative volume element) in micro or meso scale, in order to achieve the designated macro-scale material properties. To fulfill this job, computational homogenization is necessary to calculate the macro-scale properties of the RVE.

Under the level set framework, the homogenized elasticity tensor of the RVE can be calculated by Eqn. (2.3).

$$\mathbf{E}_{\bar{B}}^H = \frac{1}{|Y|} \int_D \mathbf{E}_B(\mathbf{e}^0 - \mathbf{e}(\mathbf{u}^*)) (\mathbf{e}^0 - \mathbf{e}(\mathbf{u}^*)) H(\Phi) d\Omega \quad (2.3)$$

where, \mathbf{E}_B is the elasticity tensor of the based material and $\mathbf{E}_{\bar{B}}^H$ is the homogenized elasticity tensor. $|Y|$ is the representative volume area, \mathbf{e}^0 is the applied unit strain fields, e.g. (1,0,0), (0,1,0), and (0,0,1). \mathbf{u}^* is the perturbed displacement field obtained by solving Eqn. (2.4), which is Y-period.

$$\int_D \mathbf{E}_B(\mathbf{e}^0 - \mathbf{e}(\mathbf{u}^*)) \mathbf{e}(\mathbf{v}) H(\Phi) d\Omega = 0, \quad \forall \mathbf{v} \in U \quad (2.4)$$

Therefore, to design the meta-material with specified properties, the optimization problem is formulated as follows:

$$\begin{aligned} \min. \quad & J = \frac{1}{2} (\mathbf{E}_{Bij}^H - \bar{\mathbf{E}}_{ij})^2 \\ \text{s. t.} \quad & \alpha(\mathbf{E}_B, \mathbf{u}^*, \mathbf{v}, \Phi) = l(\mathbf{v}, \Phi), \quad \forall \mathbf{v} \in U \\ & V = \int_D H(\Phi) d\Omega \leq V_{max} \\ & \alpha(\mathbf{E}_B, \mathbf{u}^*, \mathbf{v}, \Phi) = \int_D \mathbf{E}_B \mathbf{e}(\mathbf{u}^*) \mathbf{e}(\mathbf{v}) H(\Phi) d\Omega \\ & l(\mathbf{v}, \Phi) = \int_D \mathbf{E}_B \mathbf{e}^0 \mathbf{e}(\mathbf{v}) H(\Phi) d\Omega \end{aligned} \quad (2.5)$$

where, $\bar{\mathbf{E}}_{ij}$ is the target value of the homogenized \mathbf{E}_{Bij}^H .

The Lagrange multiplier method is applied to solve the optimization problem, and the adjoint method is employed to calculate the sensitivity result, where the boundary velocities can be calculated as:

$$V_n = -(\mathbf{E}_{Bij}^H - \bar{\mathbf{E}}_{ij}) \mathbf{E}_B(\mathbf{e}^0 - \mathbf{e}(\mathbf{u}^*)) (\mathbf{e}^0 - \mathbf{e}(\mathbf{u}^*)) \quad (2.6)$$

Then, the boundary velocities can be put into the Hamilton-Jacobi equation to perform the design update at an iterative basis, which belongs to the standard level set framework [12].

In Fig. 1, a few meta-material topology optimization examples are demonstrated. The based material has the Young's modulus of 1.3 and the Poisson's ratio of 0.3.

2.3 Component length scale control

As discussed earlier, component length scale control is necessary to constrain all structural member size to be bigger than some threshold value, because otherwise, the optimization result cannot be printed or suffer from the low printing quality.

Component length scale control was an extensively studied topic and the length scale control functional proposed in the author's previous work [8] is adapted to realize the length scale control effect; see Eqn. (2.7).

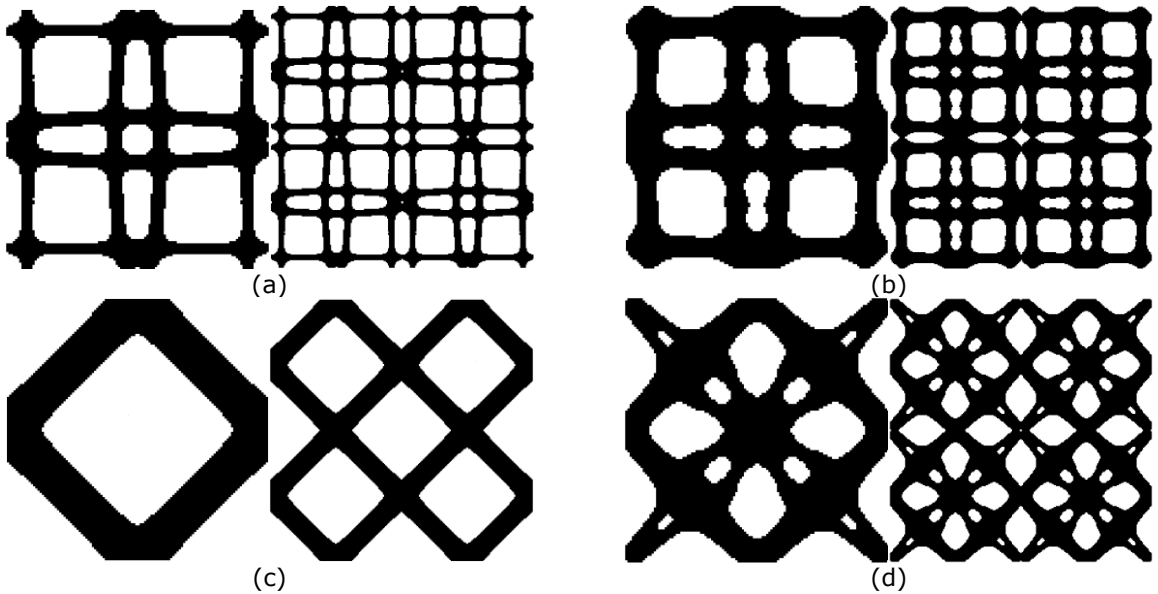


Figure 1: Examples of the meta-material topology optimization, (a) $\overline{E}_{11} = \overline{E}_{22} = 0.3$ and $V_{max} = 0.4$, the single- and 2*2 multi-unit views, (b) $\overline{E}_{11} = \overline{E}_{22} = 0.5$ and $V_{max} = 0.6$, the single- and 2*2 multi-unit views, (c) $\overline{E}_{33} = 0.14$ and $V_{max} = 0.4$, the single- and 2*2 multi-unit views (d) $\overline{E}_{33} = 0.2$ and $V_{max} = 0.6$, the single- and 2*2 multi-unit views.

$$D_T = \int_D \left\{ \left[\left(\Phi(\mathbf{X}) - \frac{\overline{T}}{2} \right)^+ \right]^2 - \left[\left(\Phi(\mathbf{X}) - \frac{\underline{T}}{2} \right)^- \right]^2 \right\} H(\Phi) d\Omega \tag{2.7}$$

The notations: $(f)^+ = \max(f, 0)$; $(f)^- = \min(f, 0)$

where \overline{T} is the upper limit of the component length scale and \underline{T} is the lower limit of the component length scale. The physical meaning of this functional is to constrain all structural member sizes to fall between the two limits.

Then, the objective function in Eqn. (2.5) is augmented into:

$$Min. \quad J(\Phi) = \frac{1}{2} (E_{Bij}^H - \overline{E}_{ij})^2 + w D_T(\Phi) \tag{2.8}$$

where w is the weight factor.

Here, only the sensitivity result of the length scale control functional is demonstrated in Eqn. (2.9), since the sensitivity result of the other part is already demonstrated in the last sub-section.

$$\frac{\partial D_T}{\partial \Phi} = \int_D G \delta(\Phi) d\Omega \tag{2.9}$$

$$G = \left[\left(\Phi(\mathbf{X}) - \frac{\overline{T}}{2} \right)^+ \right]^2 - \left[\left(\Phi(\mathbf{X}) - \frac{\underline{T}}{2} \right)^- \right]^2$$

$$+ \int_{ray_{\partial\Omega}(\mathbf{Y}) \cap \Omega} \left[2 \left(\Phi(\mathbf{Z}) - \frac{\bar{T}}{2} \right)^+ - 2 \left(\Phi(\mathbf{Z}) - \frac{\bar{T}}{2} \right)^- \right] d\mathbf{Z}$$

where \mathbf{Y} is the boundary point, $ray_{\partial\Omega}(\mathbf{Y})$ is the shortest ray connecting \mathbf{Y} to the structural skeleton, and \mathbf{Z} is the point on the ray. The details about the sensitivity derivation and the ray concept are lengthy and thus will not be demonstrated. Interested readers can refer to [8].

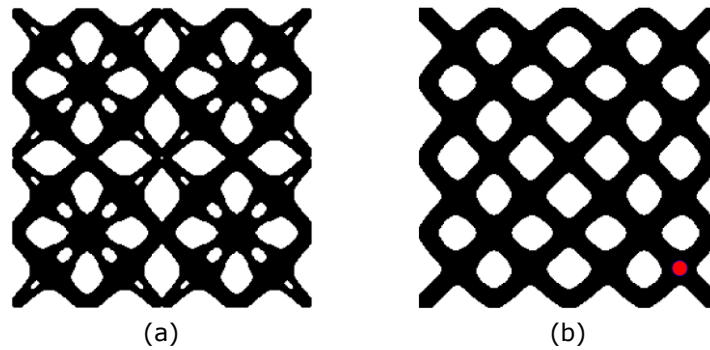


Figure 2: A comparative case study, (a) result from Fig. 1d without length scale control, (b) result with component length scale control (the red dot indicates lower limit of the component length scale).

The component length scale control is tested based on the Fig. 1d which includes many thin structural members, and the geometrically constrained result is demonstrated in Fig. 2b where the red dot indicates lower limit of the component length scale while no upper limit is applied. It can be clearly seen that the length scale requirement has been well addressed.

2.4 Curvature control to relieve stress concentration

As discussed earlier, curvature control will help round off the sharp corners and therefore reduce the stress concentration. The strength and fatigue resistance can accordingly be improved. In addition, curvature control can adjust the local curvatures based on the available cutter size so that enable post-machining to improve the sizing and surface quality.

Under the level set framework, the boundary curvature can be easily calculated by:

$$\kappa = \nabla \cdot \mathbf{n} = \nabla \cdot \left(- \frac{\nabla \Phi(\mathbf{X})}{|\nabla \Phi(\mathbf{X})|} \right) \tag{2.10}$$

So that, curvature control can be realized by adding the following constraint, where R means the radius of the curvature.

$$\kappa(\mathbf{X}) > -\frac{1}{R_1}, \text{ for any } \mathbf{X} \in \partial\Omega \tag{2.11}$$

However, it is non-trivial to calculate the sensitivity of this constraint, and thus, we inherited the idea from [7] where the curvature flow control technique is applied to address this constraint. Equation (2.12) demonstrates the curvature dependent velocities for mean curvature flow control, in which b is a positive constant. If $\kappa > 0$, the interface will move in the direction of concavity; and if $\kappa < 0$, the interface will move in the direction of convexity.

$$\mathbf{v} = -b\kappa\mathbf{n} \tag{2.12}$$

To satisfy the local curvature constraints, we need to re-define the constant b , that:

$$\begin{aligned}
 b = 0, & \quad \text{if } \kappa(X) > -\frac{1}{R} \\
 b > 0, & \quad \text{if } \kappa(X) \leq -\frac{1}{R}
 \end{aligned}
 \tag{2.13}$$

Then, the Hamilton-Jacobi equation is adapted into the convection-diffusion form, which is:

$$\phi_t + \mathbf{V} \cdot \nabla \phi = -b\kappa|\nabla \phi|
 \tag{2.14}$$

The curvature control is tested based on the Fig. 1b which includes many sharp reentrant corners (especially in the 2*2 view), and the geometrically constrained result is demonstrated in Fig. 3b where the red dot indicates lower limit of the radius of the curvature. It can be clearly seen that the curvature control constraint has been well addressed.

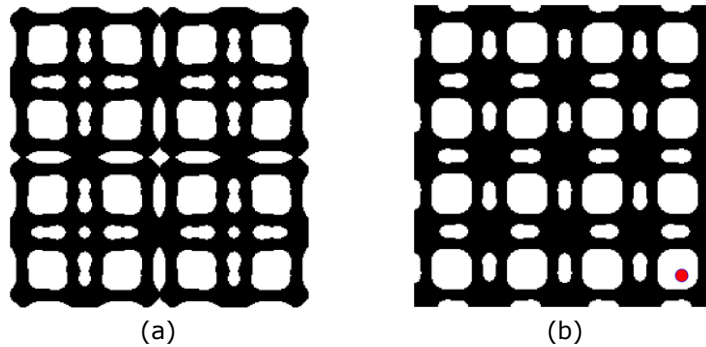


Figure 3: A comparative case study, (a) result from Fig. 1b without curvature control, (b) result with curvature control (the red dot indicates lower limit of the radius of the curvature).

3 META-MATERIAL OPTIMIZATION IN A MULTI-SCALE ENVIRONMENT

3.1 Problem formulation and solution

Generally, it is impractical to determine the targeted properties of the meta-material and, it would be more meaningful to optimize the meta-material in a part-scale circumstance, i.e., tailor the material properties based on the part's loading condition by performing multi-scale topology optimization. Note that, the multi-scale topology optimization is different from the recently popular variable-density lattice topology optimization where the latter could not allow the freeform shape and topological changes at the material level [4,5]. In this sense, the optimization problem is reformulated as below:

$$\begin{aligned}
 \text{Min.} \quad & J(\mathbf{E}^H, \mathbf{u}) = \int_{\bar{D}} \mathbf{E}^H \mathbf{e}(\mathbf{u}) \mathbf{e}(\mathbf{u}) d\Omega \\
 \text{s. t.} \quad & \alpha(\mathbf{E}^H, \mathbf{u}, \mathbf{v}) = l(\mathbf{v}), \quad \forall \mathbf{v} \in U_{ad} \\
 & \int_{\bar{D}} H(\Phi) d\Omega \leq V_{max} \\
 & \alpha(\mathbf{E}^H, \mathbf{u}, \mathbf{v}) = \int_{\bar{D}} \mathbf{E}^H \mathbf{e}(\mathbf{u}) \mathbf{e}(\mathbf{v}) d\Omega \\
 & l(\mathbf{v}) = \int_{\partial \bar{D}} \boldsymbol{\tau} \cdot \mathbf{v} dS
 \end{aligned}
 \tag{3.1}$$

where \bar{D} is the part scale design domain and D indicates the design domain of the RVE. \mathbf{E}^H is the homogenized material model following Eqn. (2.3). Note that, the level set function is only used to interpolate the material distribution within the RVE but not the macro-scale part, which means only the RVE will be designable but the part geometry will be fixed.

Similar to the last section, the Lagrange multiplier method is employed to solve this problem and the adjoint method is used to derive the sensitivity information, as shown below:

$$L' = \int_{\bar{D}} (\mathbf{E}^H)' \mathbf{e}(\mathbf{u})\mathbf{e}(\mathbf{u})d\Omega + \lambda \int_D \delta(\Phi)\Phi'd\Omega \quad (3.2)$$

$$(\mathbf{E}^H)' = -\frac{1}{|Y|} \int_D \mathbf{E}_B(\mathbf{e}^0 - \mathbf{e}(\mathbf{u}^*)) (\mathbf{e}^0 - \mathbf{e}(\mathbf{u}^*)) \delta(\Phi)\Phi'd\Omega$$

Then, if the geometric constraints are simultaneously considered, the problem formulation is further modified into:

$$\begin{aligned} \text{Min. } J(\mathbf{E}^H, \mathbf{u}) &= \int_{\bar{D}} \mathbf{E}^H \mathbf{e}(\mathbf{u})\mathbf{e}(\mathbf{u})d\Omega + w \cdot D_T \\ \text{s. t. } a(\mathbf{E}^H, \mathbf{u}, \mathbf{v}) &= l(\mathbf{v}), \quad \forall \mathbf{v} \in U_{ad} \\ &\int_D H(\Phi)d\Omega \leq V_{max} \\ \kappa(X) &> -\frac{1}{R_1}, \text{ for any } X \in \partial\Omega \end{aligned} \quad (3.3)$$

$$a(\mathbf{E}^H, \mathbf{u}, \mathbf{v}) = \int_{\bar{D}} \mathbf{E}^H \mathbf{e}(\mathbf{u})\mathbf{e}(\mathbf{v})d\Omega$$

$$l(\mathbf{v}) = \int_{\partial\bar{D}} \boldsymbol{\tau} \cdot \mathbf{v}dS$$

Sensitivity result of Eqn. (3.3) (without the curvature constraint) is presented in Eq. (3.4), and the curvature constraint is still separately solved with Eq. (2.12-2.14).

$$L' = \int_{\bar{D}} (\mathbf{E}^H)' \mathbf{e}(\mathbf{u})\mathbf{e}(\mathbf{u})d\Omega + \lambda \int_D \delta(\Phi)\Phi'd\Omega + w \int_D G\delta(\Phi)\Phi'd\Omega \quad (3.4)$$

$$(\mathbf{E}^H)' = -\frac{1}{|Y|} \int_D \mathbf{E}_B(\mathbf{e}^0 - \mathbf{e}(\mathbf{u}^*)) (\mathbf{e}^0 - \mathbf{e}(\mathbf{u}^*)) \delta(\Phi)\Phi'd\Omega$$

3.2 Numerical examples

In this sub-section, the Michell structural problem will be studied and both the component length scale control and curvature control will be implemented. In all examples, the base material has the Young's modulus of 1.3 and the Poisson's ratio of 0.3.

The initial design domain and boundary conditions are demonstrated in Fig. 4, where a force of magnitude 0.1 is loaded at the center of the bottom edge, the left foot corner is fixed and the right foot corner is clamped only in the vertical direction. The design domain size is 20*10 and the meta-material unit is meshed with a 80*80 grid. The maximum material volume fraction of the material unit is 50%.

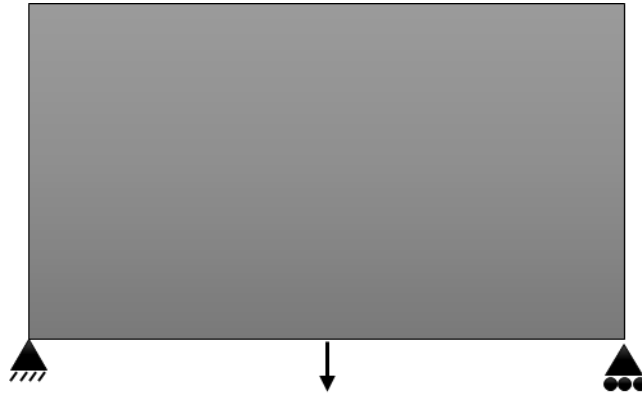


Figure 4: Problem setup of the Michell problem.

The optimization result without geometric control is shown in Fig. 5, where the final objective value is 0.2417. In addition, both the meta-material unit and the repetitively formed porous structure have been demonstrated. And if necessary, the level set field representing the meta-material structure can be post-processed into a STL file for 3D printing.

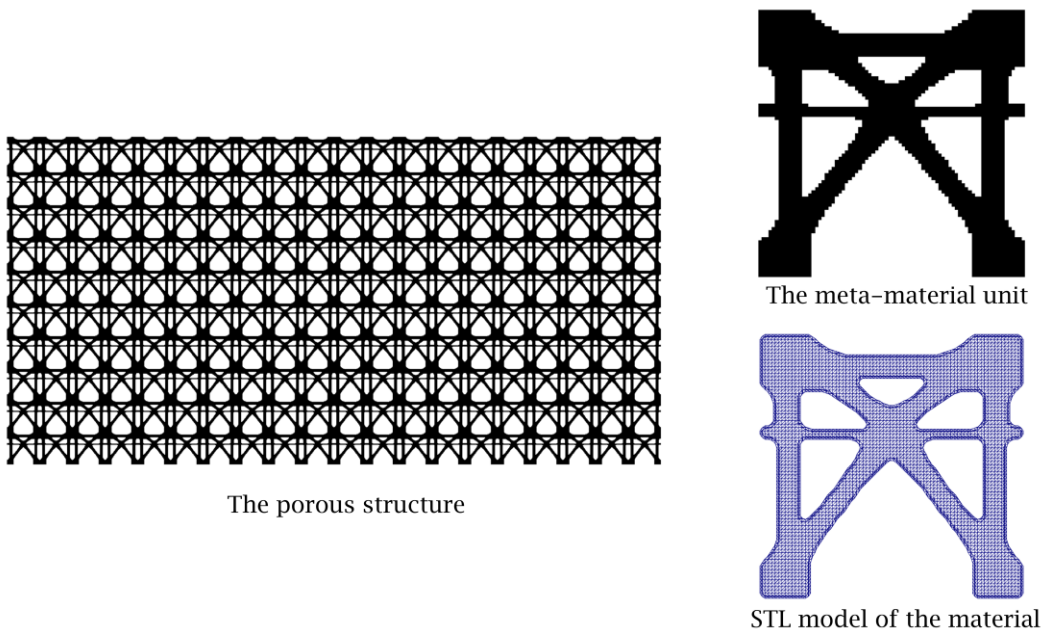


Figure 5: Michell structure optimization result without geometric control.

Then, the optimization result with component length scale control is shown in Fig. 6, where the minimum structural member size is 8 as indicated by the blue circle and apparently, the length scale control effect has been realized. Besides, the structural skeleton [8] used to realize the length scale control is also plotted out for reference. Because of the additional effort of length scale control, the objective value has been increased by 2.44% to 0.2476 as compared to the geometric control-free result.

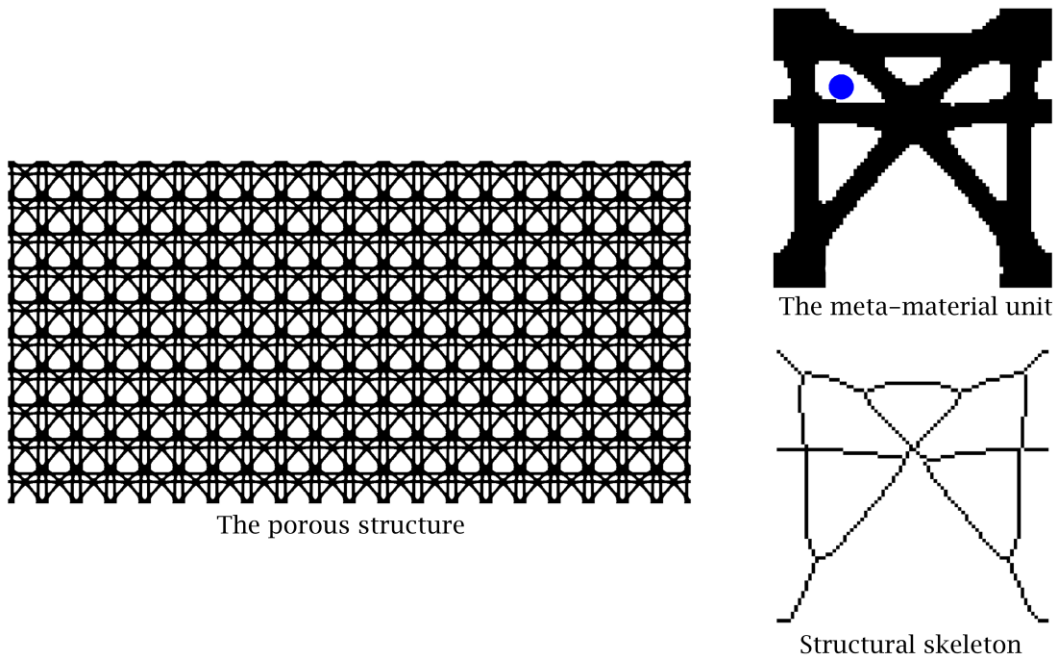


Figure 6: Michell structure optimization result with component length scale control (the blue circle indicates lower limit of the component length scale and the structural skeleton used for length scale control is also demonstrated).

The optimization result with curvature control is shown in Fig. 7, where the minimum radius of the local curvature is 5. It can be seen that the topological structure has been altered as compared to the last two results in Fig. 5 and Fig. 6. In addition, it can be clearly identified that the curvature constraint has been satisfied. Because of the additional constraint, the objective value has been increased by 3.39% to 0.2599 as compared to the geometric control-free result.

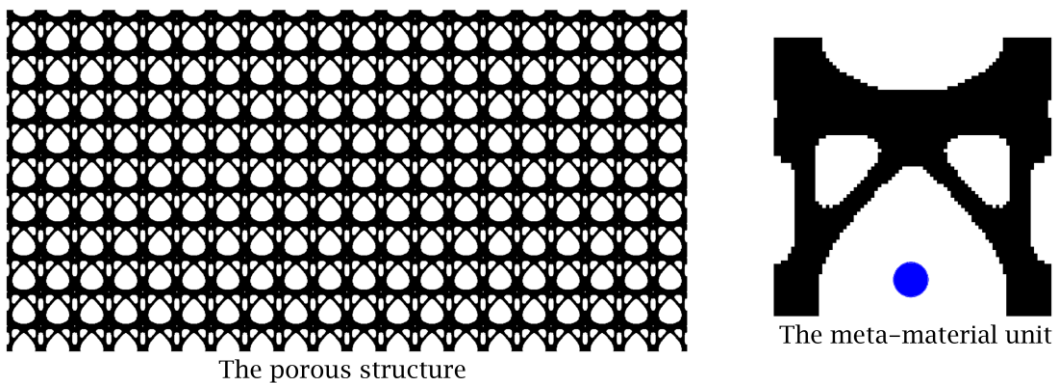


Figure 7: Michell structure optimization result with curvature control (the blue circle indicates the minimum radius of the curvature).

4 CONCLUSION

Meta-material topology optimization is studied in this article, especially the geometric control issues including component length scale control and curvature control. The part-scale application is also presented. The specific algorithm details have been demonstrated and the effectiveness have been proved through comparative case studies. In this paper, all algorithms are developed based on Matlab and implemented on a regularly-configured laptop. Since only 2D examples are studied, the computational cost is not significant where all cases can converge in minutes. For readers not familiar with the presented numerical algorithm, the published Matlab code in [14] is recommended.

Currently, the experimental study is under investigation. As known, additive manufacturing is nearly the only approach to manufacturing the meta-materials which however suffers from significant manufacturing errors that the manufactured geometry could severely deviate from the as-designed result. Hence, it would be meaningful to explore the performance deviation under different geometric control parameters.

5 ACKNOWLEDGEMENT

The project was supported by Open Research Fund of Key Laboratory of High Performance Complex Manufacturing, Central South University (Kfkt2016-07) and Natural Sciences and Engineering Research Council (NSERC) Discovery grants.

Jikai Liu, <http://orcid.org/0000-0002-9732-3791>

Jinyuan Tang, <http://orcid.org/0000-0002-6312-3855>

Rafiq Ahmad, <http://orcid.org/0000-0001-9353-3380>.

Yongsheng Ma, <http://orcid.org/0000-0002-6155-0167>

REFERENCES

- [1] Allaire, G.; Jouve, F.; Toader, A.-M.: Structural Optimization Using Sensitivity Analysis and a Level-Set Method, *Journal of Computational Physics*, 194(1), 2004, 363–393. <https://doi.org/10.1016/j.jcp.2003.09.032>
- [2] Bendsoe, M. P.; Sigmund, O.: *Topology Optimization*, Springer Berlin Heidelberg, Berlin, Heidelberg, 2004.
- [3] Challis, V. J.; Xu, X.; Zhang, L. C.; Roberts, A. P.; Grotowski, J. F.; Sercombe, T. B.: High Specific Strength and Stiffness Structures Produced Using Selective Laser Melting, *Materials & Design*, 63, 2014, 783–788. <https://doi.org/10.1016/j.matdes.2014.05.064>
- [4] Cheng, L.; Liu, J.; Liang, X.; To, A. C.: Coupling lattice structure topology optimization with design-dependent feature evolution for additive manufactured heat conduction design, *Computer Methods in Applied Mechanics and Engineering*, 332, 2018, 408–439. <https://doi.org/10.1016/j.cma.2017.12.024>
- [5] Cheng, L.; Liu, J.; To, A. C.: Concurrent lattice infill with feature evolution optimization for additive manufactured heat conduction design, *Structural and Multidisciplinary optimization*, 2018, 1–25. <https://doi.org/10.1007/s00158-018-1905-7>
- [6] Liu, J.; Ma, Y.: A Survey of Manufacturing Oriented Topology Optimization Methods, *Advances in Engineering Software*, 100, 2016, 161–175. <https://doi.org/10.1016/j.advengsoft.2016.07.017>
- [7] Liu, J.; Yu, H.; Ma, Y.: Minimum Void Length Scale Control in Level Set Topology Optimization Subject to Machining Radii, *Computer-Aided Design*, 81, 2016, 70–80. <https://doi.org/10.1016/j.cad.2016.09.007>

- [8] Liu, J.; Li, L.; Ma, Y.: Uniform Thickness Control without Pre-Specifying the Length Scale Target under the Level Set Topology Optimization Framework, *Advances in Engineering Software*, 115, 2018, 204–216. <https://doi.org/10.1016/j.advengsoft.2017.09.013>
- [9] Takezawa, A.; Kobashi, M.; Koizumi, Y.; Kitamura, M.: Porous Metal Produced by Selective Laser Melting with Effective Isotropic Thermal Conductivity Close to the Hashin–Shtrikman Bound, *International Journal of Heat and Mass Transfer*, 105, 2017, 564–572. <https://doi.org/10.1016/j.ijheatmasstransfer.2016.10.006>
- [10] van Dijk, N. P.; Maute, K.; Langelaar, M.; Van Keulen, F.: Level-set methods for structural topology optimization: a review, *Structural and Multidisciplinary Optimization*, 48(3), 2013, 437–472. <https://doi.org/10.1007/s00158-013-0912-y>
- [11] Vogiatzis, P.; Chen, S.; Wang, X.; Li, T.; Wang, L.: Topology Optimization of Multi-Material Negative Poisson’s Ratio Metamaterials Using a Reconciled Level Set Method, *Computer-Aided Design*, 83, 2017, 15–32. <https://doi.org/10.1016/j.cad.2016.09.009>
- [12] Wang, M. Y.; Wang, X.; Guo, D.: A Level Set Method for Structural Topology Optimization, *Computer Methods in Applied Mechanics and Engineering*, 192(1–2), 2003, 227–246. [https://doi.org/10.1016/S0045-7825\(02\)00559-5](https://doi.org/10.1016/S0045-7825(02)00559-5)
- [13] Wang, Y.; Luo, Z.; Zhang, N.; Kang, Z.: Topological Shape Optimization of Microstructural Metamaterials Using a Level Set Method, *Computational Materials Science*, 87, 2014, 178–186. <https://doi.org/10.1016/j.commatsci.2014.02.006>
- [14] Xia, L.; Breitkopf P.: Design of materials using topology optimization and energy-based homogenization approach in Matlab, *Structural and Multidisciplinary Optimization*, 52, 2015, 1229–1241. <https://doi.org/10.1007/s00158-015-1294-0>
- [15] Xie, Y. M.; Steven. G. P.: A simple evolutionary procedure for structural optimization, *Computers & structures* 49(5), 1993, 885–896. [https://doi.org/10.1016/0045-7949\(93\)90035-C](https://doi.org/10.1016/0045-7949(93)90035-C)
- [16] Zhang P.; Liu J.; To A. C.: Role of anisotropic properties on topology optimization of additive manufactured load bearing structures, *Scripta Materialia* 135, 2017, 148–52. <https://doi.org/10.1016/j.scriptamat.2016.10.021>